Laser-induced-fluorescence detection of collisional excitation transfer in atomic rubidium vapor during collisions with noble-gas and rubidium atoms

A. D. Sharma and H. A. Schuessler
Department of Physics, Texas A&M University, College Station, Texas 77843

R. H. Hill, Jr.
Southwest Research Institute, San Antonio, Texas 78284

(Received 24 September 1987)

The $8\,^2S$ state of rubidium is selectively populated by stepwise excitation using light from a rubidium lamp and a tunable dye laser. Excitation transfer from the $8\,^2S$ to the $6\,^2D$ state is studied in a glass cell containing rubidium vapor and noble-gas atoms at different pressures and ground-state rubidium atoms as perturbers. The thermally averaged cross sections for excitation transfer (in units of 10^{-15} cm^2) are 0.13 ± 0.05, 3.0 ± 1.2, 2.2 ± 0.9, 1.7 ± 0.7, and 4.3 ± 2.6 for the noble gases He, Ne, Ar, Kr, and Xe, respectively, and $(6.7\pm3.0)\times10^{-13}$ cm^2 for rubidium atoms. The results show that the excitation-transfer cross sections for intermediately excited states cannot be accurately scaled from simple models.

I. INTRODUCTION

Experimental studies of excitation transfer and, in particular, inelastic quenching in excited states of alkali-metal atoms have been a continuously active area of interest. Investigations of excitation transfer have been made both experimentally[1-3] and theoretically.[4-6] Recently, excitation-transfer studies were carried out in the $n=3$ and $n=4$ states of lithium,[7,8] where n is the principal quantum number. The experiments were performed mainly using excited alkali-metal atoms with parent or noble-gas atoms as perturbers. In particular, a large number of total quenching cross sections, which are the sum at all excitation-transfer cross sections from a single fine-structure state, has been measured[9] for the nS and nD states of rubidium colliding with helim for intermediate n values ($9\leq n\leq 18$). More recent measurements[10] extended this work to the high-n region ($32\leq n\leq 45$) for nS states colliding with He, Ne, Ar, and Xe. For the high-lying Rydberg states, the valence electron is only loosely bound and the collision of the alkali-metal atom and the noble-gas atom can be described by the scattering of a free electron with a noble-gas atom. Clearly, this procedure must become progressively less valid as one looks at the collisions of atomic states having lower values for the principal quantum number.

In the experiment described here, we have explored this low-n region by observing excitation transfer from the $8\,^2S_{1/2}$ state of rubidium induced by the noble-gas atoms of He, Ne, Ar, Kr, Xe, and Rb. However, rather than measuring the overall quenching cross section for the nonradiative decay of the $8\,^2S_{1/2}$ state into all possible other states, one particular channel of the reaction, in which the final state is the $6\,^2D$ state, was investigated. The reaction can be represented as

$$8\,^2S_{1/2}+X\rightarrow 6\,^2D+X\ ,$$

where X stands for any one of the inert noble-gas atoms He, Ne, Ar, Kr, and Xe, or ground-state rubidium atoms. The excitation-transfer reaction studied is a major channel in the quenching of the $8\,^2S_{1/2}$ state, since there is near resonance between the separation of the $8\,^2S_{1/2}$ and the $6\,^2D$ levels ($\Delta E=357$ cm^{-1}) and the value of kT at 150 °C (294 cm^{-1}), the temperature at which the experiment was performed.

II. EXPERIMENT

The experimental arrangement is similar to the one used in our previous fine-structure-changing collision studies.[11-13] A glass cell containing rubidium vapor was constantly pumped by a VacIon pump (5 l/sec) to a background pressure of less than 10^{-6} Torr. Then the pump was turned off and a small amount of a noble gas was introduced into the cell. An absolute-pressure measurement was carried out using a capacitance manometer (Baratron Model 227) which was calibrated with a McLeod gauge and argon gas. The manometer measured absolute pressures from about 10^{-3} to a maximum of 1 Torr and is insensitive to the nature of the noble gas. The pressure range used in our experiment was between 0.1 and 1 Torr for Ne, Ar, Kr, and Xe. However, much higher pressures were required to observe excitation-transfer collisions with helium. In the latter case, the pressure measurement was carried out using a mercury-column manometer which was buffered by a cold trap filled with liquid nitrogen. The rubidium vapor pressure was controlled by heating a small sidearm of the glass resonance bulb with silicone oil maintained at the constant temperature of 115 °C. The main body of the bulb was kept at 150 °C by an additional heater to prevent condensation of rubidium vapor on the cell walls. The temperatures of both the sidearm and the cell body were constantly monitored with Chromel-Alumel thermocouples.

Figure 1 illustrates the excitation and observation scheme. In the first step, light from a rubidium radio-frequency (rf) lamp excited rubidium atoms to the $5\,^2P_{1/2}$ state using the first resonance line at 7948 Å. In the second step, light from a multimode dye laser (Spectra Physics Model 375) transferred rubidium atoms from the intermediate $5\,^2P_{1/2}$ state to the final $8\,^2S_{1/2}$ state, when the laser was tuned to 6071 Å. A laser power of about 100 mW was obtained employing Rhodamine 6G as the dye and pumping it with 4 W of 5145-Å light from an argon-ion laser. The laser bandwidth of 20 GHz was comparable to the Doppler width of 15 GHz and was produced by inserting both a tuning wedge and a thin étalon into the laser cavity. Fluorescence was observed at three wavelengths, namely, 6160 Å ($8\,^2S_{1/2} \rightarrow 5\,^2P_{3/2}$), 6206 Å ($6\,^2D_{3/2} \rightarrow 5\,^2P_{1/2}$), and 6298 Å ($6\,^2D_{5/2} \rightarrow 5\,^2P_{3/2}$). A photomultiplier (EMI 9658R) in conjunction with a lock-in amplifier (PAR Model 124 A) were employed for detection. The exciting light from the rf lamp in the first step was chopped at the lock-in amplifier reference frequency of 35 Hz, to discriminate against the directly scattered laser light at 6071 Å in the second step. Discrimination against the light at 7948 Å was obtained with a monochromator whose slit width was fixed at 0.5 mm. The resolution of the monochromator was approximately 10 Å.

The various fluorescence signals were recorded at a series of noble-gas pressures for He, Ne, Ar, Kr, and Xe. Figure 2 shows such recorder traces for the Rb-Xe collision system, as an example. The fluorescence intensities

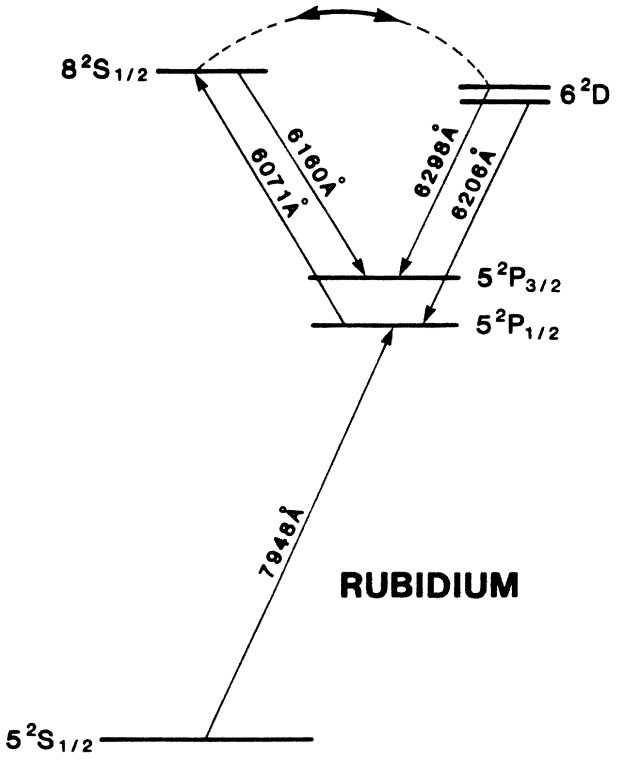

FIG. 1. Partial energy diagram of the Rb atom involved in the stepwise excitation and fluorescence emission scheme.

I_C at 6298 Å ($6\,^2D_{5/2} \rightarrow 5\,^2P_{3/2}$) and I_B at 6206 Å ($6\,^2D_{3/2} \rightarrow 5\,^2P_{1/2}$) are a direct measure of the population of the $6\,^2D_{5/2,3/2}$ states. Excitation-transfer cross sections were determined from these fluorescence signals when they were normalized to the transition I_A at 6160 Å ($8\,^2S_{1/2} \rightarrow 5\,^2P_{3/2}$). This was possible since the $6\,^2D$ states were predominantly and directly populated from the $8\,^2S_{1/2}$ state by nonradiative excitation-transfer collisions. The results are plotted in Fig. 3 for the relative fluorescence intensity at $\lambda = 6298$ Å. A similar but less accurate graph was obtained for our measurement at $\lambda = 6206$ Å. Our analysis neglects second-order processes due to collisions through intermediate states because these processes must necessarily give a much smaller contribution than the direct $8\,^2S_{1/2} \rightarrow 6\,^2D$ collision channel. No significant polarization effects have been observed with the present experimental arrangement. Therefore, it was concluded that, over the pressure range studied, the strong collisional effects completely masked possible small polarization effects.

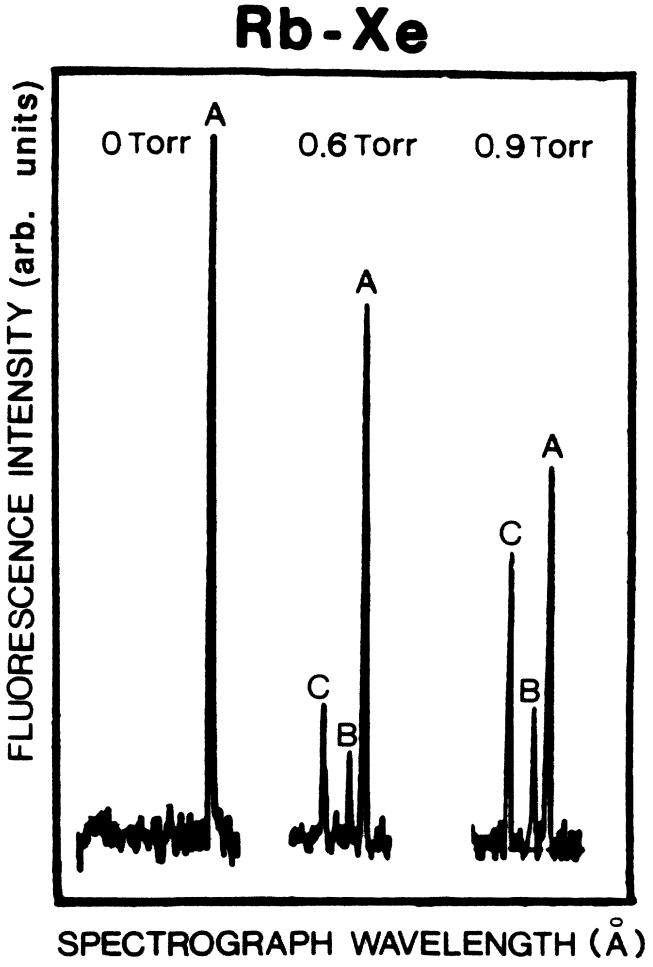

FIG. 2. Fluorescent-light intensity as a function of the monochromator wavelength for excitation by the light from the (rf) lamp ($\lambda = 7948$ Å) and the fixed laser frequency ($\lambda = 6071$ Å) and three different xenon pressures: *A*, $8\,^2S_{1/2} \rightarrow 5\,^2P_{3/2}$ ($\lambda = 6160$ Å); *B*, $6\,^2D_{3/2} \rightarrow 5\,^2P_{1/2}$ ($\lambda = 6206$ Å); *C*, $6\,^2D_{5/2} \rightarrow 5\,^2P_{3/2}$ ($\lambda = 6298$ Å).

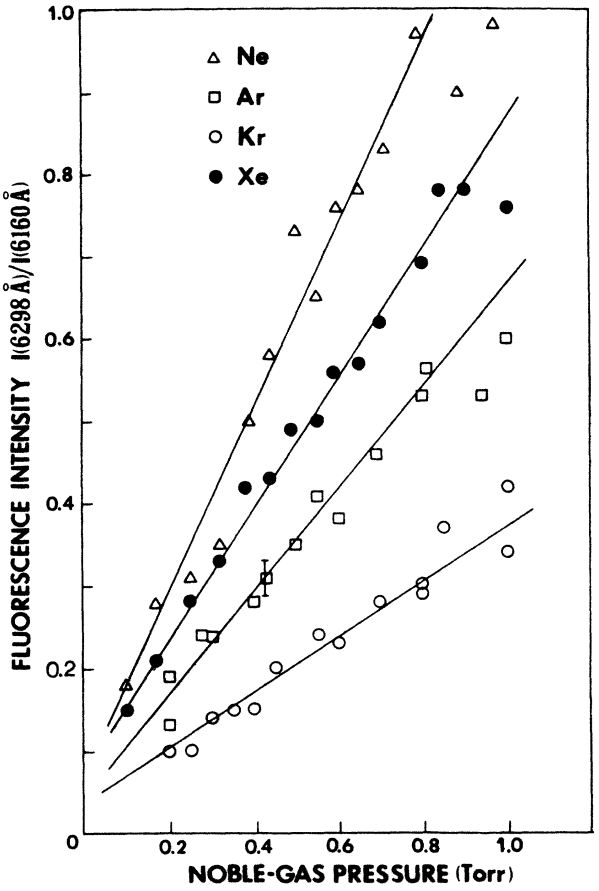

FIG. 3. Observed fluorescent-light intensity ratios $I_C(6\,^2D_{5/2})/I_A(8\,^2S_{1/2})$ vs the noble-gas pressure for Ne, Ar, Kr, and Xe.

III. RATE EQUATIONS

In equilibrium, the production rate of atoms into the $6\,^2D$ states is due mainly to collisions with Rb atoms in the $8\,^2S_{1/2}$ state with noble-gas perturbers, but contains also contributions due to collisions with other partners; for instance, Rb atoms in both the ground and excited states. The loss rate from the $6\,^2D$ states consists of radiative processes and collisional transfers out of the doublet. Thus, the production rate into the $6\,^2D$ states is

$$dN_{6D}/dt = NN_{8S}\bar{v}\sigma_l + N^*N_{8S}\bar{v}^*\sigma_l^* + N\sum_{\substack{i\\ i\neq 8S}} \bar{v}N_i\,{}^i\sigma_l + N^*\sum_{\substack{i\\ i\neq 8S}} \bar{v}^*N_i\,{}^i\sigma_l^* , \quad (1)$$

where N_{6D} is the Rb $6\,^2D$ state density, N_{8S} is the Rb $8\,^2S_{1/2}$ state density, N or N^* is the Rb ground-state density or the noble-gas density, N_i is the density of the ith state of Rb. $\bar{v}$ or $\bar{v}^*$ is the relative average velocity between excited Rb and ground-state Rb atoms or noble-gas atoms, and σ_l or σ_l^* is the thermally averaged cross section for excitation transfer from the $8\,^2S_{1/2}$ state into the $6\,^2D$ states due to collisions with Rb ground-state or noble-gas atoms. The loss rate from the $6\,^2D$ states is described by

$$-dN_{6D}/dt = N_{6D}\left[1/\tau_{6D} + \sum_i N_i\bar{v}\,{}^i\sigma_{\rm tr} + N^*\bar{v}^*\sigma_{\rm tr}^*\right] , \quad (2)$$

where the additional symbols are ${}^i\sigma_{\rm tr}$, the transfer cross section out of the $6\,^2D$ state by a collision with Rb atoms in state i; and τ_{6D}, the radiative lifetime of the $6\,^2D$ state, which includes all radiative processes, such as stimulated emission due to blackbody background radiation.[13] At equilibrium, the production rate equals the loss rate, yielding

$$NN_{8S}\bar{v}\sigma_l + N^*N_{8S}\bar{v}^*\sigma_l^* + N\sum_{\substack{i\\ i\neq 8S}} N_i\bar{v}\,{}^i\sigma_l + N^*\sum_{\substack{i\\ i\neq 8S}} N_i\bar{v}^*\,{}^i\sigma_l^* = N_{6D}\left[1/\tau_{6D} + \sum_i N_i\bar{v}\,{}^i\sigma_{\rm tr} + N^*\bar{v}^*\sigma_{\rm tr}^*\right] . \quad (3)$$

In the present experiment, the $8\,^2S_{1/2}$ state is continuously populated by laser excitation, hence the first two terms on the left-hand side of Eq. (3) dominate the production terms. The second two terms involve multiple collisions and can be neglected with respect to the first two terms at the moderate-to-low rubidium and noble-gas densities used. The loss terms on the right-hand side of Eq. (3) were all considered in the analysis; however, the second term, which involves collisional transfer out of the $6\,^2D$ state due to collisions with other Rb states, was dominated by collisions with ground-state atoms and can be rewritten as

$$N_{6D}\sum_i N_i\bar{v}\,{}^i\sigma_{\rm tr} \approx N_{6D}N\bar{v}\sigma_{\rm tr} . \quad (4)$$

Taking this into account, we can reduce Eq. (3) to

$$\frac{N_{6D}}{N_{8S}} = \frac{N\bar{v}\sigma_l + N^*\bar{v}^*\sigma_l^*}{(1/\tau_{6D} + N\bar{v}\sigma_{\rm tr} + N^*\bar{v}^*\sigma_{\rm tr}^*)} . \quad (5)$$

Since not the density ratio N_{6D}/N_{8S} but the related fluorescence ratio

$$I_C(\lambda = 6298\ \text{Å})/I_A(\lambda = 6160\ \text{Å})$$

was observed, the relation between the two must be calculated and is given as

$$I_C/I_A = f_1 N_{6D}/N_{8S} , \quad (6a)$$

where f_1 is a combination of Einstein factors A and weighting factors $g(j)$, with j being the total angular momentum of the state,

$$f_1 = \frac{[A(6\,^2D_{5/2}\rightarrow 5\,^2P_{3/2})g(\frac{5}{2}) + A(6\,^2D_{3/2}\rightarrow 5\,^2P_{3/2})g(\frac{3}{2})]/[g(\frac{5}{2})+g(\frac{3}{2})]}{A(8\,^2S_{1/2}\rightarrow 5\,^2P_{3/2})} . \quad (6b)$$

The Einstein A factors were derived from the oscillator strengths given by Migdalek and Baylis[14] calculated using relativistic Hartree-Fock theory with core polarization. For the transitions of interest, these oscillator strengths agree within 4% with those more recently published by Hansen.[15] However, when the same comparison was made for other transitions not used in the present experiment, discrepancies of up to 25% were found. We therefore believe that our results may still have a small systematic error due to an uncertainty in the calculation of the A factors. For the evaluation of the present experiment, the following A factors were used:

$$\begin{aligned} &A(8\,^2S_{1/2}\rightarrow 5\,^2P_{3/2})=2.21\times 10^6\ \text{sec}^{-1}\ , \\ &A(6\,^2D_{5/2}\rightarrow 5\,^2P_{3/2})=3.12\times 10^6\ \text{sec}^{-1}\ , \\ &A(6\,^2D_{3/2}\rightarrow 5\,^2P_{3/2})=0.525\times 10^6\ \text{sec}^{-1}\ , \\ &A(6\,^2D_{3/2}\rightarrow 5\,^2P_{1/2})=2.44\times 10^6\ \text{sec}^{-1}\ . \end{aligned} \tag{7}$$

For the relative intensity I_C/I_A, Eqs. (5) and (6) were combined with Eq. (7) to yield

$$\frac{I_C}{I_A}=\left[\frac{1}{f_1}\right]\left[\frac{N\bar{v}\sigma_l+N^*\bar{v}^*\sigma_l^*}{1/\tau_{6D}+N\bar{v}\sigma_{\text{tr}}+N^*\bar{v}^*\sigma_{\text{tr}}^*}\right], \tag{8}$$

where, according to Eq. (6b), $f_1=1.06$. Similarly, for completeness, for the relative intensity I_B/I_A of the weaker doublet line I_A at $\lambda=6206$ Å, we obtain

$$\frac{I_B}{I_A}=\left[\frac{1}{f_2}\right]\left[\frac{N\bar{v}\sigma_l+N^*\bar{v}^*\sigma_l^*}{1/\tau_{6D}+N\bar{v}\sigma_{\text{tr}}+N^*\bar{v}^*\sigma_{\text{tr}}^*}\right], \tag{9}$$

where we calculated $f_2=2.26$ analogously to Eq. (6b). It should be noted that in Eqs. (8) and (9), the fluorescence ratio was measured as a function of $N^*\bar{v}^*$ at constant $N\bar{v}$. Therefore, these equations can be used to calculate the energy-transfer cross sections σ_l^* and σ_l that are of interest.

A further check on the reliability of the Einstein A factors was carried out by measuring intensity ratios, such as I_C/I_B, in the high-pressure limit of several Torr noble gas. In this limit, these ratios depend only on combinations of A factors and statistical weights and agree, to within a few percent, with the calculated values.

IV. DATA ANALYSIS AND RESULTS

In the low-pressure regime, the data compiled in Fig. 3 show for a given temperature a linear dependence on the noble-gas pressure and therefore also on the noble-gas density N^*. Expanding, for instance, Eq. (8) around $N^*\bar{v}^*=0$, yielded

$$\frac{I_C}{I_A}\approx\frac{1}{f_1}\left[\frac{a}{c}+\left[\frac{b}{c}-\frac{da}{c^2}\right]N^*\bar{v}^*\right], \tag{10}$$

where

$$a=N\bar{v}\sigma_l,\quad b=\sigma_l^*,\quad c=1/\tau_{6D}+N\bar{v}\sigma_{\text{tr}},\quad d=\sigma_{\text{tr}}^*\ .$$

A similar linear equation holds in approximating Eq. (9).

The y intercept and slope of Eq. (10) were determined using standard least-squares-fitting procedures. The first term is the y intercept and yielded the energy-transfer cross section σ_l for collisions with Rb ground-state atoms. The slope dependence on N^* is expressed in the second term, and the slope contains the energy-transfer cross section σ_l^* for collisions with noble-gas atoms. In this connection, we have also employed the values for the transfer cross section σ_{tr} for Rb-Rb collisions $\sigma_{\text{tr}}=3.8\times 10^{-13}$ cm^2 and for Rb–noble-gas collisions σ_{tr}^* which are known from our previous work.[12] Both σ_{tr} and σ_{tr}^* have been corrected for the fact that we use the relative average velocity in the present work, whereas, previously, other definitions for the velocity (such as v_{rms}) were employed. The rubidium density N as derived from Nesmeyanov's equation[16] for the cold-finger temperature of 115 °C is $N=1.22\times 10^{13}$ cm^{-3}. The relative average velocity $\bar{v}$ between the rubidium and the noble gas is calculated according to $\bar{v}=\sqrt{8RT/\pi\mu}$, where R is the gas constant, μ is the reduced mass, and $T=150$ °C is the temperature in the main cell. The radiative lifetime[17] of the $6D$ state is $\tau=237$ ns, with a detailed discussion of the reasoning for using this value having been outlined previously.[13]

The results of our measurements for the thermally averaged energy-transfer cross sections σ_l^* for the various noble gases are compiled in Table I. We have derived the values for the transfer cross sections from our I_C/I_A data and have used the I_B/I_A measurement merely for checking consistency. The reasons are that the A factor for I_C, the transition from the $6\,^2D_{5/2}$ state to the $5\,^2P_{3/2}$ state, is nearly six times larger than the A factor for I_B, the transition from the $6\,^2D_{3/2}$ state to the $5\,^2P_{1/2}$ state [Eq. (7)]. Due to this difference, secondary collisions, which further complicate the analysis, are six times less likely. Additionally, the statistical weighting factor of the $6\,^2D_{5/2}$ state is larger by a factor of 1.5 than that of the $6\,^2D_{3/2}$ state, so that the light intensity at I_C is approximately nine times stronger than at I_B.

It should also be noted that the various parameters and their associated errors, which enter into Eq. (8), influence the calculation of σ_l^* in a nontrivial way. The values of σ_{tr}^*, as well as those of $\bar{v}^*$, are different for each buffer gas. Therefore, the cross sections of interest do not simply scale as do the slopes of the curves in Fig. 3.

The results for the thermally averaged energy-transfer cross sections from the $8S$ to the $6D$ state, σ_l, for ground-state rubidium atoms are also listed in Table I. Since a value for σ_l was determined for each buffer gas, the value quoted is the average of these values, with the error representing the standard deviation.

TABLE I. Compilation of energy-transfer cross sections, σ_l^*, for Rb $8\,^2S_{1/2}$ in collisions with noble-gas atoms and σ_l with ground-state Rb atoms (in units of 10^{-15} cm^2).

Element	I_C/I_A
He	0.13±0.05
Ne	3.0 ±1.2
Ar	2.2 ±0.9
Kr	1.7 ±0.7
Xe	4.3 ±2.6
Rb	670 ±300

TABLE II. Experimental values for energy-transfer (σ_l^*) and quenching (σ_Q) cross sections for selected states in rubidium in collisions with noble-gas atoms (in units of cm^2).

State	He	Ne	Ar	Kr	Xe
σ_l^*[Rb($8S \rightarrow 6D$)] ($\Delta E = 357.43\ cm^{-1}$)	$(0.13\pm0.05)\times10^{-15}$ [a]	$(3.0\pm1.2)\times10^{-15}$ [a]	$(2.2\pm0.9)\times10^{-15}$ [a]	$(1.7\pm0.7)\times10^{-15}$ [a]	$(4.3\pm2.6)\times10^{-15}$ [a]
σ_Q[Rb(12S)]	$(1.10\pm0.20)\times10^{-14}$ [b]				
σ_Q[Rb(14S)]	$(2.15\pm0.50)\times10^{-14}$ [b]				
σ_Q[Rb(16S)]	$(1.45\pm0.40)\times10^{-14}$ [c]				$(2.6\pm0.5)\times10^{-12}$ [b]
σ_Q[Rb(18S)]	$(3.25\pm0.65)\times10^{-14}$ [c]				
σ_Q[Rb(27S)]					6.6×10^{-13} [g]
σ_Q[Rb(9F)]	$(8.70\pm1.75)\times10^{-14}$ [c]		$(1.30\pm0.30)\times10^{-13}$ [c]		$(4.60\pm1.40)\times10^{-13}$ [c]
σ_Q[Rb(11F)]	$(1.05\pm0.20)\times10^{-13}$ [c]		$(3.90\pm0.80)\times10^{-13}$ [c]		$(8.80\pm2.70)\times10^{-13}$ [c]
σ_Q[Rb(13F)]	$(1.00\pm0.20)\times10^{-13}$ [c]		$(3.50\pm0.70)\times10^{-13}$ [c]		$(1.30\pm0.40)\times10^{-12}$ [c]
σ_Q[Rb(15F)]	$(8.10\pm1.60)\times10^{-13}$ [c]		$(2.50\pm0.50)\times10^{-13}$ [c]		$(2.00\pm0.70)\times10^{-12}$ [c]
σ_Q[Na(9S)]	$7.3(10)\times10^{-16}$ [d]		$18.9(30)\times10^{-16}$ [d]		$29(6)\times10^{-16}$ [d]
σ_Q[Na(10S)]	$14.4(30)\times10^{-16}$ [d]		$18.1(30)\times10^{-16}$ [d]		$56(9)\times10^{16}$ [d]
σ_Q[Na(11S)]	$21(5)\times10^{-16}$ [d]				$97(20)\times10^{-16}$ [d]
σ_l^*Li($3P \rightarrow 3D$) $\Delta E = 357.7\ cm^{-1}$	8.6×10^{-16} [e]	1.1×10^{-16} [e]			
σ_l^*[Li($4D \rightarrow 4F$)] $\Delta E = 6.8\ cm^{-1}$	$(1.20\pm0.25)\times10^{-14}$ [f]		$(1.90\pm0.50)\times10^{-14}$ [f]		

[a]This work ($T = 150$ °C).
[b]Reference 9 ($T = 247$ °C).
[c]Reference 18 ($T = 247$ °C).
[d]Reference 19 ($T = 152$ °C).
[e]Reference 7 ($T = 590 - 635$ °C).
[f]Reference 8 ($T = 602 - 627$ °C).
[g]Reference 20 (beam).

V. DISCUSSION

Only a few excitation-transfer cross sections into a single atomic state have been observed for the alkali-metal atoms. However, a large number of quenching cross sections, which are the sum of all excitation-transfer cross sections out of a particular state, are known. In Table II, we therefore compare our results to these values, which may be considered as upper limits. On a crude scale, the size of the cross sections is inversely proportional to the energy difference between the two states involved. This explains the smaller values of the cross sections for low-n states as compared to the cross sections for high-n states. The helium cross sections are always smaller than the ones for xenon. The helium cross section measured in the present experiment is reasonably small. The value obtained is approximately 45 times smaller than the corresponding value for xenon. A similar observation[9] was made for the quenching cross section from the $16S$ state in rubidium where this ratio is nearly 180. On a finer scale, no clear trends of the size of the cross sections on simple atomic parameters exist. This indicates that excitation transfer into intermediately excited states depends critically on the potential curves of each particular collision molecule. The situation is analogous to that described by Nikitin,[21] who used alkali-metal noble-gas potential curves to calculate fine-structure-changing collisions. Considering the relative motion of the alkali-metal and noble-gas atoms, the electrostatic (polarization or exchange) forces will, at a certain distance, create a competition with magnetic spin-orbit coupling. In addition, at shorter internuclear distances, the magnetic spin-orbit interaction competes with the Coriolis interactions. In comparison, the various collision processes are much better described theoretically for high-Rydberg atoms ($n \geq 15$) and noble-gas atoms. There, Matsuzawa[22] shows the dependence of the cross sections on only two atomic parameters, namely, the noble-gas polarizability and the zero-energy electron–noble-gas scattering length.

Table III presents a compilation of our rubidium-rubidium energy-transfer cross section and known quenching cross sections. In these alkali-metal–alkali-metal types of collisions, the long-range dipole-dipole interaction dominates the process. For the Rydberg states with $12 \leq n \leq 18$, the quenching cross sections roughly follow the geometrical cross sections σ_g. The presently measured energy-transfer cross section of the intermediately excited $8S$ state can also be seen to be of the same order of magnitude as the geometrical cross section.[25] A linear extrapolation of the listed quenching cross sections on a semilogarithmic scale accounts for the n^2 dependence, and yielded an estimate for the quenching cross section in the $8S$ state of $\sigma_Q = 4.4 \times 10^{-13}$ cm^2. The size of this estimate is similar to the value of the related energy-transfer cross section σ_l obtained in the present experiment.

TABLE III. Experimental values for energy-transfer (σ_l) and quenching (σ_Q) cross sections from nS states of Rb in collisions with ground-state Rb atoms. The geometrical cross sections (σ_g) are included for comparison.

Cross section	Value (cm^2)	σ_g (cm^2)
$\sigma_l[\mathrm{Rb}(8\,^2S_{1/2} \rightarrow 6\,^2D]$[a]	$(6.7 \pm 3.0) \times 10^{-13}$	1.24×10^{-13}
$\sigma_Q[\mathrm{Rb}(12S)]$[b]	$(1.4 \pm 0.4) \times 10^{-12}$	1.35×10^{-12}
$\sigma_Q[\mathrm{Rb}(14S)]$[b]	$(2.10 \pm 0.45) \times 10^{-12}$	3.05×10^{-12}
$\sigma_Q[\mathrm{Rb}(16S)]$[c]	$(3.9 \pm 1.0) \times 10^{-12}$	6.00×10^{-12}
$\sigma_Q[\mathrm{Rb}(18S)]$[b]	$(7.0 \pm 1.4) \times 10^{-12}$	1.07×10^{-11}
$\sigma_Q[\mathrm{Rb}(34 \leq nS \leq 43)]$[d]	$(\sim 2) \times 10^{-11}$	$\sim \times 10^{-10}$

[a]This work ($T = 150$ °C).
[b]Reference 23.
[c]Reference 18.
[d]Reference 24.

VI. CONCLUSION

In this paper we have presented experimental results of a series of measurements of energy-transfer collisions from the $8\,^2S$ to the $6\,^2D$ states of rubidium. The measurements were carried out with the various noble-gas and ground-state rubidium atoms as perturbers. While for such intermediately excited states, the order of magnitude of the cross section can be reasonably explained using energy arguments involving the energy difference between the states and the geometrical cross sections,[13,15] a more accurate prediction of the cross section requires a theory which, for each specific collision pair, considers detailed knowledge of the form of the potential-energy curve between the excited alkali-metal atom and the ground-state perturbers.

ACKNOWLEDGMENTS

This work was supported by the National Science Foundation under Grant No. PHY81-11943, the Robert A. Welch Foundation, and the Center for Energy and Mineral Resources of Texas A&M University. One of the authors (R.H.H.) received support from the Advisory Committee for Research, Southwest Research Institute, Internal Research Project No. 15-9451.

[1]J. Cuvelier, P. R. Fournier, F. Gounand, J. Pascale, and J. Bernande, Phys. Rev. A **11**, 836 (1975).
[2]J. M. Mestdagh, J. Cuvelier, J. Berlande, A. Bivet, and P. DePujo, J. Phys. B **13**, 4589 (1980).
[3]M. Glodz, J. B. Atkinson, and L. Krause, Can. J. Phys. **59**, 548 (1981).
[4]M. Krauss, P. Maldonado, and A. C. Wahl, J. Chem. Phys. **54**, 4944 (1971).
[5]W. E. Baylis, J. Chem. Phys. **51**, 2665 (1969).
[6]J. Pascale and J. Vandeplanque, J. Chem. Phys. **60**, 2278 (1974).
[7]C. Chaleard, B. Dubrevil, and A. Catherinot, Phys. Rev. A **26**, 1431 (1982).
[8]B. Dubrevil and C. Chaleard, Phys. Rev. A **29**, 958 (1984).

[9]M. Hugon, F. Gounand, P. R. Fournier, and J. Berlande, J. Phys. B **13**, 1585 (1980).
[10]M. Hugon, B. Sayer, P. R. Fournier, and F. Gounand, J. Phys. B (to be published).
[11]R. H. Hill, Jr., H. A. Schuessler, and B. G. Zollars, Phys. Rev. A **25**, 834 (1982); R. H. Hill, Jr., Ph.D. thesis, Texas A&M University, 1979.
[12]B. G. Zollars, H. A. Schuessler, J. W. Parker, and R. H. Hill, Jr., Phys. Rev. A **28**, 1329 (1983).
[13]J. W. Parker, H. A. Schuessler, R. H. Hill, Jr., and B. G. Zollars, Phys. Rev. A **29**, 617 (1984).
[14]8. Migdalek and W. E. Baylis, Can. J. Phys. **57**, 1708 (1979).
[15]W. Hansen, J. Phys. B **17**, 4883 (1984).
[16]A. N. Nesmeyanov, *Vapor Pressure of the Elements* (Academic, New York, 1963).
[17]J. Marek and P. Münster, J. Phys. B **13**, 1731 (1980).
[18]M. Hugon, F. Gounand, P. R. Fourier, and J. Berlande, J. Phys. B **12**, 2707 (1979).
[19]T. F. Gallagher and W. E. Cooke, Phys. Rev. A **19**, 2161 (1979).
[20]L. N. Goeller, G. B. McMillan, K. A. Smith, and F. B. Dunning, Phys. Rev. A **30**, 2756 (1984).
[21]E. E. Nikitin, *Theory of Elementary Atomic and Molecular Processes in Gases* (Clarendon, Oxford, 1974).
[22]M. Matsuzawa, J. Phys. B **12**, 3743 (1979).
[23]M. Hugon, F. Gounand, and P. R. Fournier, J. Phys. B **13**, L109 (1980).
[24]M. Hugon, F. Gounand, P. R. Fournier, and J. Berlande, J. Phys. B **16**, 2531 (1983).
[25]H. Bethe and E. E. Salpeter, *Quantum Mechanics of One and Two Electron Atoms* (Plenum, New York, 1977).